Meiotic arrest occurs most frequently at metaphase and is often incomplete in azoospermic men

Andrea Enguita-Marruedo, Ph.D.,[a] Esther Sleddens-Linkels, B.Sc.,[a] Marja Ooms, B.Sc.,[a] Vera de Geus, B.Sc.,[a] Martina Wilke, B.Sc.,[b] Eric Blom, Ph.D.,[b] Gert R. Dohle, M.D., Ph.D.,[c] Leendert H. J. Looijenga, Ph.D.,[d,g] Wiggert van Cappellen, Ph.D.,[e] Esther B. Baart, Ph.D.,[f] and Willy M. Baarends, Ph.D.[a]

[a] Department of Developmental Biology, [b] Department of Clinical Genetics, [c] Department of Urology, [d] Department of Pathology, [e] Department of Pathology/Erasmus Optical Imaging Centre, and [f] Department of Obstetrics and Gynaecology, Erasmus MC, University Medical Center Rotterdam; and [g] Princess Maxima Center for Pediatric Oncology, Utrecht, The Netherlands

Objective: To establish which meiotic checkpoints are activated in males with severe spermatogenic impairment to improve phenotypic characterization of meiotic defects.
Design: Retrospective observational study.
Setting: University medical center research laboratory and andrology clinic.
Patient(s): Forty-eight patients with confirmed spermatogenic impairment (Johnsen scores 3–6) and 15 controls (Johnsen score 10).
Intervention(s): None.
Main Outcome Measure(s): Quantitative assessment of immunofluorescent analyses of specific markers to determine meiotic entry, chromosome pairing, progression of DNA double-strand break repair, crossover formation, formation of meiotic metaphases, metaphase arrest, and spermatid formation, resulting in a novel classification of human meiotic arrest types.
Result(s): Complete metaphase arrest was observed most frequently (27%), and the patients with the highest frequency of apoptotic metaphases also displayed a reduction in crossover number. Incomplete metaphase arrest was observed in 17% of the patients. Only four patients (8%) displayed a failure to complete meiotic chromosome pairing leading to pachytene arrest. Two new types of meiotic arrest were defined: premetaphase and postmetaphase arrest (15% and 13%, respectively).
Conclusion(s): Meiotic arrest in men occurs most frequently at meiotic metaphase. This arrest can be incomplete, resulting in low numbers of spermatids, and often occurs in association with reduced crossover frequency. The phenotyping approach described here provides mechanistic insights to help identify candidate infertility genes and to assess genotype-phenotype correlations in individual cases. (Fertil Steril® 2019;112:1059–70. ©2019 by American Society for Reproductive Medicine.)
El resumen está disponible en Español al final del artículo.

Key Words: Meiotic arrest, meiosis, nonobstructive azoospermia, infertility, spermatogenesis

The quality of the haploid (epi) genome of a male germ cell depends on the activity of checkpoint mechanisms during spermatogenesis. These should induce apoptosis of aberrant germ cells. Meiosis is a particularly risky subphase of spermatogenesis because it involves induction and repair of around 200 DNA double-strand breaks (DSBs) that are required for proper chromosome pairing and crossover formation (1). In mouse and man, these DSBs are marked by accumulation of phosphorylated histone H2AX (γH2AX) (2, 3), resulting in a nucleus-wide spreading of many overlapping patches of γH2AX signal upon immunostaining in early meiotic prophase cells (leptotene and zygotene). As DSB repair and chromosome pairing progress, this signal declines, and the synaptonemal complex (the protein complex that connects the

Received March 22, 2019; revised June 28, 2019; accepted August 6, 2019.
A.E.-M. has nothing to disclose. E.S.-L. has nothing to disclose. M.O. has nothing to disclose. V.d.G. has nothing to disclose. M.W. has nothing to disclose. E.B. has nothing to disclose. G.R.D. has nothing to disclose. L.H.J.L. has nothing to disclose. W.v.C. has nothing to disclose. E.B.B. has nothing to disclose. W.M.B. has nothing to disclose.
A.E.-M and W.M.B. were supported by the European Commission through EU-FP7-PEOPLE-2011-ITN289880. The funders had no role in study design, data collection and analysis, decision to publish, or preparation of the manuscript.
Reprint requests: Willy M. Baarends, Ph.D., Room Ee902a, Department of Developmental Biology, Erasmus MC, University Medical Center, P.O. Box 2040, 3000 CA Rotterdam, The Netherlands (E-mail: w.baarends@erasmusmc.nl).

Fertility and Sterility® Vol. 112, No. 6, December 2019 0015-0282

https://doi.org/10.1016/j.fertnstert.2019.08.004

axes of chromosomes) forms (reviewed in Zickler and Kleckner [1]). This process is called synapsis and can be followed by immunolocalization of synaptonemal complex components such as synaptonemal complex protein 3 (SYCP3), allowing the identification of the different substages of meiotic prophase: leptotene, zygotene, pachytene, and diplotene. When the synaptonemal complex is completely formed, pachytene is reached. However, the X and Y chromosome synapse only partially, due to lack of homology in regions outside the so called pseudoautosomal region, and γH2AX concentrates on this DNA to facilitate formation of the transcriptionally silenced chromatin structure named the XY body at the onset of pachytene (4, 5). In general, most of the induced DSBs are repaired as noncrossovers, and only a minority form crossovers (around 10%–20%, depending on the species). During pachytene, crossovers are specifically marked by accumulation of the mismatch repair protein MLH1 (6, 7). At least one crossover per chromosome pair is required to ensure proper segregation of chromosomes at the first meiotic metaphase-to-anaphase transition (1). Once the cells reach metaphase, chromosomes accumulate phosphorylation of histone H3 at serine 10 (H3S10ph), and this marker can be used to identify cells at this relatively brief stage (8).

Several meiotic checkpoints that operate during spermatogenesis have been described for mice (9–14). First, the so-called pachytene checkpoint eliminates spermatocytes in which chromosome synapsis is incomplete, and this is functionally coupled to a failure to form the XY body in male mice (14). In addition, a second checkpoint operates during pachytene, sensing DNA damage (15, 16). If repair and chromosome pairing occur normally, the next checkpoint ensures correct segregation of chromosomes at the metaphase-to-anaphase transition. This spindle assembly checkpoint (SAC) functions in both mitosis and meiosis and senses correct attachment of each chromosome to the spindle. Anaphase only occurs after the SAC is satisfied (11, 17–19).

In infertile men, occurrence of meiotic arrest phenotypes has been described, and estimations of the percentage of oligo- or azoospermic patients with meiotic arrest vary between 10% and 30% (20–28). In addition, detailed analyses of different meiotic parameters, such as progression of chromosome pairing and crossover formation, have been performed in such patients (3, 21, 29–31). More recently, RNA sequencing analyses have also been used to characterize a small group of selected azoospermic patients (32). However, in general, arrest phenotypes in azoospermic or severely oligospermic men remain poorly characterized and very few genetic causes of nonobstructive azoospermia in men (often involving consanguinous families) have been identified (33–36).

Here we aimed to obtain more insight into the types, frequency, and completeness of meiotic arrest in men displaying severe spermatogenic impairment. We hypothesize that if spermatogenic impairment is caused by genetic factors, this will often lead to specific activation of one of the above-described meiotic checkpoints and associated specific types of meiotic arrest. To assess meiotic arrest in relation to checkpoint activation, we set out to validate protein markers that could be used for reliable identification of cells arrested at different stages of spermatogenesis by immunofluorescent staining of paraffin-embedded testis biopsy samples.

MATERIALS AND METHODS

Patient Inclusion and Genetic and Pathological Results

This study used remnant paraffin-embedded testis biopsy material from azoospermic or severely oligospermic patients or from patients for whom testicular malignancy was suspected. Material was collected from 462 patients between 2001 and 2013. The testis biopsies had been fixed in 4% paraformaldehyde and embedded in paraffin. In these biopsies, the pathology laboratory routinely analyzes histological patterns and uses the quantitative histological grading system developed by Johnsen (37) to assess spermatogenesis. In brief, the level of sperm maturation is graded between 1 and 10, according to the most advanced germ cell in the tubule, in at least 100 seminiferous tubules. Analyses of *AZF* deletions and/or common *CFTR* mutations and/or karyotyping were performed as described (38).

Surplus fixed biopsy samples were selected for the current analysis, and we excluded the sample when [1] a malignancy was reported in the biopsy, [2] the patient was known to carry sex chromosome aberrations, [3] routine Johnsen score (JS) (37) assessment was lacking and there was also no mention of "maturation arrest" by the pathologist, and [4] no leftover material was available.

Ethics Approval

The use of surplus tissue samples was approved by the local Institutional Review Board of the Erasmus MC Rotterdam (METC 02.981). This included the permission to use the secondary tissue without further consent. Samples were used according to the Code for Proper Secondary Use of Human Tissue in The Netherlands developed by the Dutch Federation of Medical Scientific Societies (FMWV, http://www.federa.org/, version 2002, update 2011). This is a retrospective study that was anonymized.

Fluorescent Immunohistochemistry

Testis biopsies were sectioned (6 μm) and placed on a drop of demineralized H_2O (dH_2O) on slides (Starfrost). After stretching the sections on a heating plate at 39°C, slides were dried overnight at 37°C. Subsequently, slides were placed at 60°C for 1 hour. Then the slides were dewaxed and rehydrated as follows: 3 × 5 minutes xylene, 3 × 5 minutes 100% ethanol, and 3 × 5 minutes phosphate-buffered saline (PBS). The slides were then incubated for 15 minutes in Proteinase K in PBS (1 μg/mL). This was followed by washing steps with dH_2O (4 × 2 minutes) and an incubation with terminal deoxynucleotidyl transferase buffer (0.1 M Na-cacodylate, pH 6.8, 1.0 mM CoCl, 0.1 mM DTT) for 30 minutes in a humid chamber. Subsequently, the slides were washed 3 × 5 minutes with TB buffer (300 mM NaCl, 30 mM tri-sodiumcitrate-dihydrate in dH_2O) and 3 × 5 minutes with dH_2O. Thereafter, an epitope retrieval step was performed with sodium citrate buffer pH 6

(1 mM trisodium citrate [dihydrate]) + 0.05% (v/v) Tween 20 (Sigma-Aldrich) in a microwave at maximum power (1 × 10 minutes, 2 × 5 minutes, whereby after each microwave incubation period, the initial volume was restored by adding dH^2O). The slides were cooled down to room temperature in the sodium citrate buffer for 1 hour and washed with PBS (3 × 5 minutes). Blocking was performed by incubating the sections in 10% normal goat serum and 5% bovine serum albumin (BSA) diluted in PBS, in a humid chamber for 30 minutes at room temperature. When we used dual fluorescent staining, we performed sequential immunostaining rounds for each primary antibody and its associated secondary, fluorescent-tagged antibody, to reduce the risk of secondary antibody cross reaction. Thus, in the first round, the first primary antibody (diluted in 5% BSA/PBS) was added to the sections, and the slides were incubated in a humid chamber at 4°C overnight. The second day, the slides were kept at room temperature for 1 hour and then washed 3 × 5 minutes with PBS. Subsequently, the appropriate secondary antibody (diluted in PBS) was added and the slides were incubated for 1.5 hours in a humid chamber at room temperature. After washing (3 × 5 minutes) in PBS, incubation with the second primary antibody in 5% BSA/PBS followed overnight. On the third day, we repeated the steps for addition of the appropriate secondary antibody for the most recently added primary antibody to allow detection of the associated antigen. Finally, slides were washed 3 × 5 minutes in PBS and mounted using Prolong Gold Antifade reagent with DAPI.

Antibodies

Rabbit polyclonal anti-SYCP3 (noncommercial antibody described in Lammers et al. [39]) at 1:10,000, mouse monoclonal anti-MLH1 (cat. 551091, BD Pharmingen) at 1:25, mouse polyclonal anti-γH2AX at 1:10,000 (Millipore, 05-636), rabbit polyclonal anti-H3Ser10ph at 1:1,000 (06-570, Millipore), and mouse acrosome-specific antibody at 1:100 (noncommercial antibody described in Moore et al. [40]) were used. For secondary antibodies, we used goat anti-rabbit alexa 488 IgG and goat anti-mouse alexa 546 IgG (A-11008 and A-11003, respectively; Invitrogen), both at 1:500 dilution.

Analyses of Fluorescent Immunostainings of Human Testis Biopsy Sections

Quantitative analyses of meiotic entry, XY body formation, and spermatid formation were performed at 200× or 1,000× magnification on an Axioplan 2 Carl Zeiss fluorescence microscope, equipped with a digital camera (Coolsnap-Pro; Photometrics). Only round tubules were scored (defined as tubules whereby the longest and shortest diameter differed by less than two-fold). A minimum of 50 random round tubules was evaluated per patient. On samples stained with anti-γH2AX and anti-H3ser10ph the number of tubules that contained at least one early cell was counted to determine the percentage of early cell positive tubules (1,000× magnification, EC+T). The same analysis was performed for the XY body, to determine the percentage of XY body positive tubules (200× magnification, XY+T). In addition, the number of XY bodies per XY body–positive tubule was assessed at 1,000× magnification. The percentage of tubules that contain spermatids and the most advanced spermatid stage reached were determined on slides immunostained with the acrosome-specific antibody (1,000× magnification, SPT+T).

Quantitative analyses of (apoptotic) metaphases were performed using a 63× oil immersion Plan-Apochromat objective, Zeiss LSM700 confocal microscope equipped with a digital camera (Axiocam MRm Rev.3 1388X1040). To obtain the percentage of apoptotic metaphases, all metaphases in a section were scored on samples stained with anti-γH2AX and anti-H3ser10ph and classified as apoptotic if they were also clearly positive for γH2AX immune signal (bright green signal; care was taken to ensure separation of the red fluorescent signal (H3S10ph, alexa 546) from the green fluorescent signal (γH2AX, alexa 488). The total number of metaphases was normalized to the area analyzed (metaphases/mm^2), and the percentage of apoptotic metaphases was also calculated.

For counting MLH1 foci, Z-stacks from at least five different spermatocytes were made per patient (63× objective and 5× digital zoom). These Z-stacks were merged into two-dimensional images (maximum projection). The number of MLH1 foci was counted using the "Find Maxima" function of the Image J software (41). The noise tolerance was set manually. For each patient the average number of MLH1 foci per spermatocyte was then calculated.

Threshold Calculations

To establish baseline frequencies of tubule cross sections containing cells at a specific spermatogenic stage, we determined the normal range in our control samples for the following variables: percentage early cell positive tubules (%EC+T), percentage XY body positive tubules (%XY+T), the number of XY bodies per XY body positive tubule (XY/XY+T), the number of metaphases/mm^2, the percentage of metaphases that show apoptosis, and the number of MLH1 foci per nucleus. The values observed for each variable in control patients were averaged, and the SDs were calculated. The normal range was determined using the mean ± 2 SD (95% confidence interval), which then served as threshold values. For %EC+T and %XY+T, the lowest control value was not inside the 95% confidence interval, and in these cases, this lowest control value was used as the threshold, since a Grubb's test did not classify these as outliers. Finally, an additional threshold for the number of metaphases/mm^2 was established by calculating the mean and SD values from the patients for whom no XY bodies were observed (groups I and II); then we set the minimal threshold value for reaching meiotic metaphases at this mean +2 SD. Table 1 shows an overview of mean values and normal ranges. In all cases, absence of more advanced stages indicated cell arrest at or around the most advanced spermatogenic stage that still could be observed.

RESULTS

Patients

From 307 patients included in this study (see Materials and Methods for criteria), 74 (24%) were assigned a JS below 3,

TABLE 1

Mean values and normal range of meiotic parameters.

Quantitative parameter	Mean ± SD value in controls	Normal range/thresholds
% of tubules containing cells in early meiotic prophase	88.2 ± 18.6	100–43.9[a]
% of tubules containing XY body–positive nuclei	96.5 ± 4.5	100–82.6[a]
No. of XY body–positive nuclei/XY body–positive tubule	20.2 ± 6.2	32.6–7.74
No. of metaphases/mm^2	7.54 ± 2.5	12.54–2.53
Minimal metaphases/mm^2 for meiotic metaphases		>1.83[b]
% of apoptotic metaphases	4.6 ± 3.4	0–11.5
No. of MLH1 foci	40.8 ± 5.8	52.4–29.3

Note: SD = standard deviation.
[a] Threshold corresponds to the lowest value in controls (no outlier).
[b] Value based on mean + 2 SD metaphases/mm^2 in group I and group II patients.

Enguita-Marruedo. Meiotic metaphase arrest in men. Fertil Steril 2019.

48 (16%) patients had JS 3–6, 67 (22%) had JS 7–8, 35 (11%) displayed variability of >2 in JS between left and right testis biopsy, and 83 (27%) had JS 9–10. The 48 patients with JS 3–6 (including four patients for whom no JS was available but maturation arrest was indicated by the pathologist) were selected (see Supplemental Table 1 for available information). In addition, 15 patients with JS 10 were randomly chosen and used as controls. In total, 35 of the selected patients and controls (JS 3–6 and JS 10, respectively) had also been analyzed for *AZF* deletions and/or common *CFTR* mutations and/or karyotype. Aberrations were found in five JS 3–6 patients: a pericentric inversion in chromosome 1 (P13; 46,XY,inv(1)(p21q32.1)), a balanced translocation between the long arm of the Y-chromosome and the long arm of chromosome 19 (P35; 46,X,t(Y;19)(q12;q13.3)), two *AZFc (DAZ)* deletions (P10 and P17), and a heterozygote carrier of a *CFTR* mutation (P41 (R117H/7T)). From the group of the JS 10 controls, one had been analyzed for genetic aberrations, and this patient (C13) carried two *CFTR* mutations: 1717-1G>A and Q1476X, most likely explaining the obstructive azoospermia in this patient.

Validation of Protein Markers and Classification of Meiotic Arrest Patients

We optimized an immunofluorescent staining protocol (see Materials and Methods for details) to assess meiotic progression in archived paraffin-embedded and formaldehyde-fixed biopsy material. We used a double immunostaining of anti-phosphorylated H2AX (γH2AX) and anti-phosphorylated H3 (H3Ser10ph) to assess whether checkpoint activation and associated arrest occurred in the JS 3–6 patients: γH2AX, marking meiotic DSBs and the XY body, was used to verify entry into meiosis, progression of DSB repair, and XY body formation (as a proxy for completion of synapsis and repair). These are important parameters to assess activation of the two pachytene checkpoints. Figure 1A shows low-magnification overviews of part of a tubule section containing early spermatocytes (leptotene and zygotene, marked by the presence of multiple γH2AX patches) and a section containing pachytene nuclei with a clear XY body. In addition, H3Ser10ph immunostaining was used to identify M-phase cells, and metaphases were identified by the combination of this signal with a metaphase plate appearance of the DNA (visualized by DAPI staining; Fig. 1B). Occasionally, metaphases also displayed intense γH2AX signal along the condensed chromosomes. Since this type of panchromosomal γH2AX staining has been described as a hallmark of cells entering apoptosis (42), we classified these aberrant metaphases as apoptotic (Fig. 1B, apoptotic metaphase). This proved to be a very useful parameter to identify patients with a meiotic metaphase arrest (see below).

Round, elongating, and condensing spermatids could be reliably observed at low magnification using an antibody that labels the acrosome, in combination with the DAPI signal (Fig. 1C), and five subtypes were identified using higher magnification (Supplemental Fig. 1A). Similarly, substages of meiotic prophase could also be more clearly distinguished at higher magnification, based on the pattern of γH2AX staining (Supplemental Fig. 1B).

We quantified meiotic entry, XY body formation, and (apoptotic) metaphases for the patients and controls. In addition, the presence and most advanced type of spermatids were scored. We set thresholds for each parameter (Fig. 1D–1G, Table 1) as described in Materials and Methods and interpreted the results by developing a decision tree (Fig. 1H). First, we verified whether spermatogenesis progressed up to formation of meiotic DSBs (presence of early spermatocytes, Fig. 1A, 1D). If this was not the case, arrest is likely to be premeiotic, or very early meiotic, with a failure to induce meiotic DSBs (group I). The next step was to determine whether pachytene was reached as evidenced by XY body formation, the hallmark of completion of both synapsis and DSB repair (Fig. 1A, 1E). If XY bodies were not detected, this would indicate activation of one of the two pachytene checkpoints, and these patients were classified as group II. After assessing the metaphase density in the whole patient group, we observed a clear positive correlation between the number of metaphases/mm^2 and the number of XY bodies per XY+T (R^2 = 0.35; $P<.0001$; Fig. 1F), confirming that formation of an XY body is a prerequisite for metaphase entry. For group I and II patients, all observed metaphases are expected to be of mitotic origin. Thus, the values obtained for these two groups of patients (group I: failure to enter meiosis; and group II: failure to form the XY body) were used to define a threshold of 1.83 metaphases/mm^2, above which we consider additional

FIGURE 1

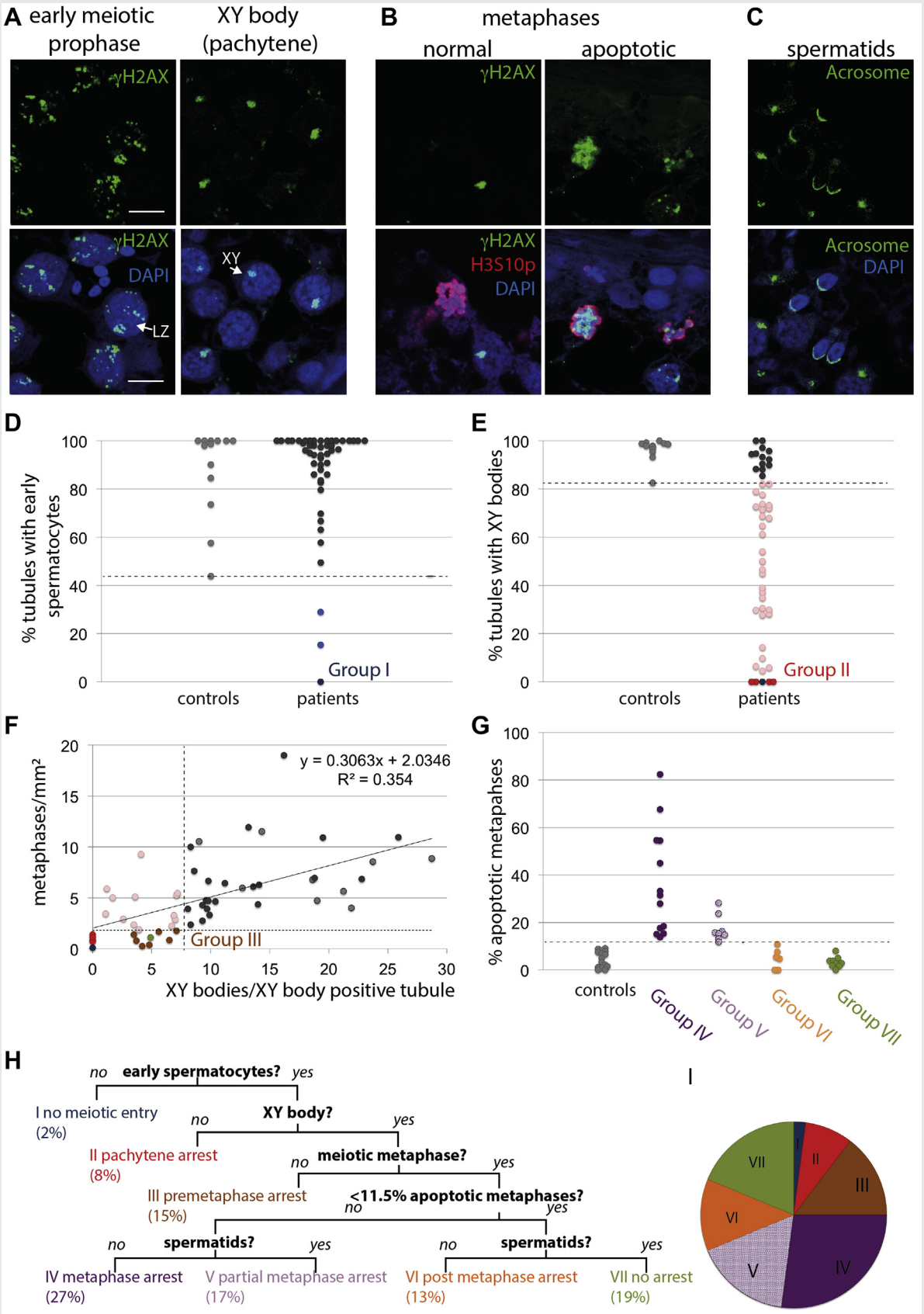
A early meiotic prophase
XY body (pachytene)
B metaphases
normal
apoptotic
C spermatids
γH2AX
Acrosome
DAPI
XY
LZ
H3S10p
D
% tubules with early spermatocytes
Group I
controls
patients
E
% tubules with XY bodies
Group II
F
metaphases/mm²
y = 0.3063x + 2.0346
R² = 0.354
Group III
XY bodies/XY body positive tubule
G
% apoptotic metapahses
Group IV
Group V
Group VI
Group VII
H
early spermatocytes?
I no meiotic entry (2%)
XY body?
II pachytene arrest (8%)
meiotic metaphase?
III premetaphase arrest (15%)
<11.5% apoptotic metaphases?
spermatids?
IV metaphase arrest (27%)
V partial metaphase arrest (17%)
VI post metaphase arrest (13%)
VII no arrest (19%)
I

metaphases to be of meiotic origin (Table 1 and Supplemental Table 1). We identified eight patients that displayed a metaphase density below this threshold. These patients also displayed a reduced capacity to reach pachytene (Fig. 1F, brown dots). For one of these patients, P46 (Fig. 1F, green dot), we detected occasional spermatids in 38% of the tubules; Supplemental Table 1), indicating that some cells were still able to proceed through metaphase I and complete meiosis. This patient was therefore classified as showing no arrest (group VII). No spermatids were detected in the other seven patients, and these were therefore classified as having a premetaphase arrest (group III).

Next we assessed for the rest of the patients whether the percentage of apoptotic meiotic metaphase cells was increased compared with the normal range we established in the control group (Table 1, Fig. 1G), and used this as measure of meiotic metaphase arrest. We then used the absence or presence of spermatids in the tubules to classify these patients as having a complete metaphase arrest (group IV) or an incomplete metaphase arrest (group V). We also observed that some patients did not show any sign of known checkpoint activation, but where spermatids were completely lacking, we classified these as postmetaphase arrest (group VI). In the remaining patients we observed spermatids and no indications of checkpoint activation and classified these as no arrest (group VII).

The frequencies of patients classified in each group is shown in Figure 1I, and typical examples of immunostaining patterns for each class are shown in Supplemental Figure 2. Only four cases (8%) displayed complete activation of the pachytene checkpoints (failure to form the XY body, group II), while 44% displayed complete (27%, group IV) or partial metaphase arrest (17%, group V), likely due to activation of the SAC. In addition to the previously described pachytene and metaphase arrests, we were able to define two additional types of arrest: premetaphase and postmetaphase arrest (15% [group III] and 13% [group VI], respectively). More detailed descriptions of the criteria and specific aspects of the phenotypes are outlined below for each group.

Meiotic Entry

The vast majority of patients displayed normal percentages of tubules with early spermatocytes (%ES+T; Fig. 1D, Supplemental Table 1). The single group I patient (P10, dark blue dot in Fig. 1D) was one of the two patients that carried an *AZFc* deletion. Two patients (P4 and P18) showed a reduction in %ES+T, based on the set normal range (Fig. 1D, light blue dots). Based on the other assessed parameters, and following the decision tree, these were subsequently classified into group IV and V, respectively (Supplemental Table 1).

XY Body Formation and Activation of Pachytene Checkpoint

In line with a failure to enter meiosis, no tubules containing XY bodies were found in the group I patient with no meiotic entry (P10). Four additional patients displayed a complete lack of XY bodies (Fig. 1E, red dots), and thus their spermatocytes were unable to reach the pachytene stage normally. This indicates activation of either the synapsis-dependent or DSB repair–dependent pachytene checkpoint (group II). Further analysis of meiotic prophase in the four patients with pachytene arrest revealed that the spermatocytes of P3 and P33 entered meiotic prophase normally, but groups of cells arrested at leptotene or early zygotene. In contrast, only isolated early spermatocytes where detected in P7 and P25, but these appeared to have progressed further into zygotene, based on the pattern of γH2AX (Fig. 2A, 2B).

Twenty-nine patients scored below the normal range of percentage of XY body-positive tubules (XY+T; Fig. 1E, pink dots, and Supplemental Table 1). To obtain a more sensitive assessment of the efficiency of progression to pachytene, independent of meiotic entry, we also assessed the number of XY bodies per XY+T. This parameter showed a strong positive correlation to the percentage of XY+T as expected ($R^2 = 0.53$; $P<.0001$; Fig. 2C). In patients with a reduced number (<7.7) of XY bodies per XY+T, spermatocytes reach pachytene with reduced efficiency. This points to cell loss at some point between meiotic entry and pachytene.

Meiotic Metaphase and Activation of the SAC

Other than a reduced capacity to reach pachytene (Fig. 1F and Fig. 2C), we observed no specific aberrant feature that could explain the failure to reach meiotic metaphase for group III patients, except for spermatocytes of P44, which often displayed panchromosomal γH2AX staining (Fig. 2D). As described above for the apoptotic metaphases, this is a hallmark of apoptosis and provides an explanation for the loss of spermatocytes in this patient.

Twenty-one patients displayed an increased percentage of apoptotic metaphases compared with controls (Fig. 1G), indicating frequent activation of the SAC, leading to apoptosis. Most of these patients also displayed a reduced

Quantitative assessment of progression of meiosis in paraffin-embedded testis sections. (**A**) Immunostaining of early meiotic prophase and pachytene spermatocytes (control sample). (**B**) Normal (control patient) and apoptotic (patient displaying metaphase arrest) metaphase nuclei. (**C**) Spermatids (control sample). Magnifications of the indicated late zygotene (LZ) and pachytene (XY) nucleus are shown in Supplemental Figure 1B. Scale bar, 10 μm. (**D**) Percentage of tubules that contain early spermatocytes and (**E**) percentage of tubules that contain XY bodies in controls and JS 3–6 patients. The dark blue dot in panel D indicates the group I patient, and light blue dots indicate patients with values below the threshold. Red dots in panel E indicate group II patients, and pink dots indicate JS 3–6 patients with values below the threshold. (**F**) Correlation between the number of XY bodies per XY+T and the number of metaphases/mm^2 ($P<.0001$). Dark brown dots indicate group III patients, and the green dot indicates one group VII patient with a value below the threshold for reaching meiotic metaphase. (**G**) Further classification of patients depending on the percentage of apoptotic metaphases and the presence/absence of spermatids. Color codes as indicated. (**H**) Decision tree for the classification of patients; percentages and colors correspond to the pie diagram shown in panel I.

Enguita-Marruedo. Meiotic metaphase arrest in men. Fertil Steril 2019.

FIGURE 2

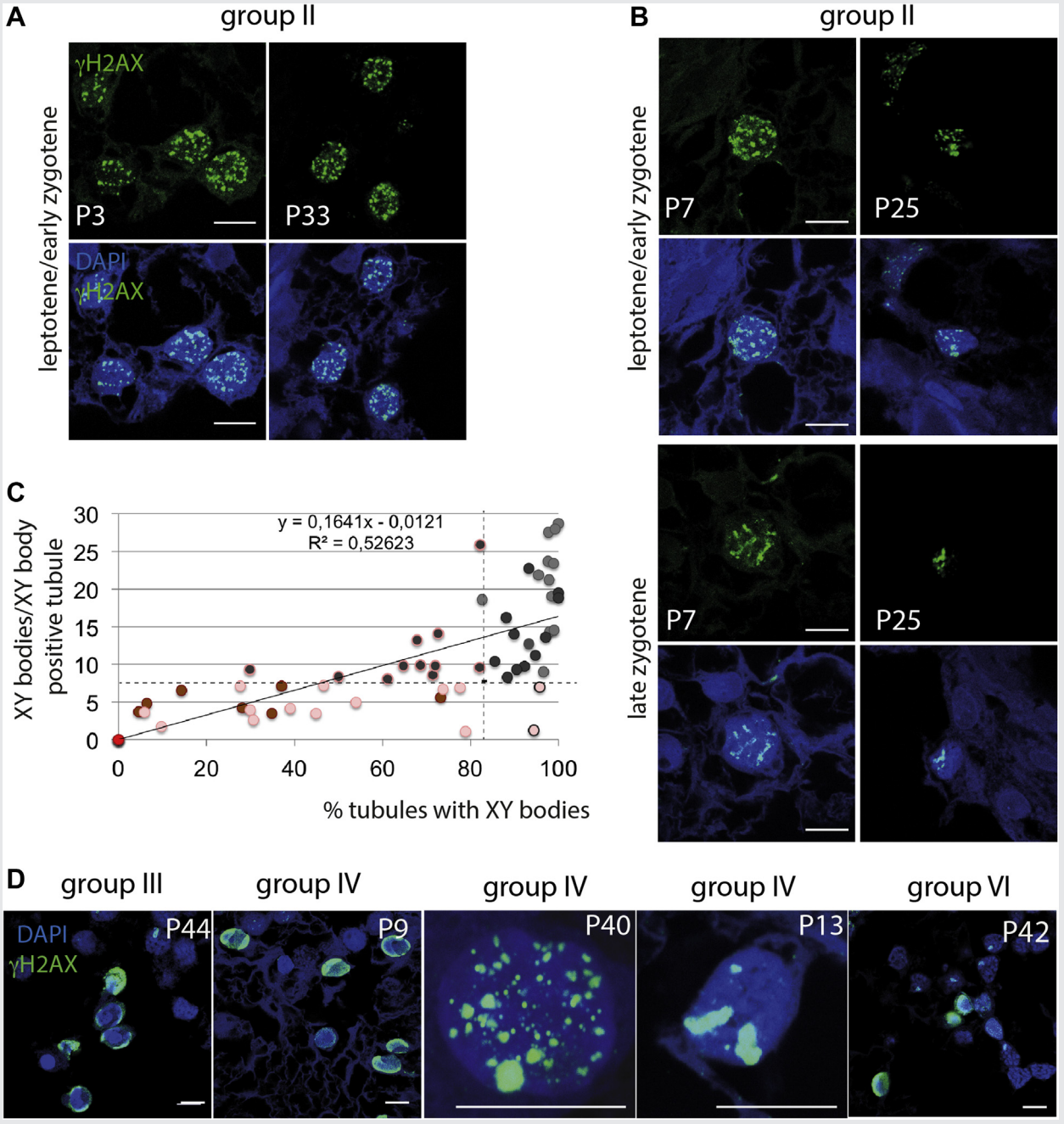

Efficiency of XY body formation and aberrations in γH2AX pattern in spermatocytes of group II, III, IV, and VI patients. (**A** and **B**) Aberrations in the γH2AX pattern (green staining) in samples of patients displaying failure to form the XY body (pachytene arrest, group II). Intriguingly, the spermatocyte nuclei of P25 were half the size of the nuclei observed in the other three patient biopsies in this group. This could indicate a gross alteration in nuclear/chromatin structure in the spermatocytes of this patient, but fixation artefacts cannot be excluded. (**C**) Positive correlation between the percentage of tubules with XY bodies and the number of XY bodies per XY+T. Red dots (four on top of each other) indicate group II patients; pink dots and brown dots (all group III patients) are patients for whom both parameter values were below the threshold; pink dots with dark gray outlines represent values whereby only the number of XY bodies per XY+T was reduced; and dark gray dots with pink outlines only display a reduced percentage of tubules with XY bodies. Dark gray dots represent all JS 3–6 patients who displayed values within the normal range for both parameters, and light gray dots represent the controls. (**D**) Representative images of aberrant γH2AX staining in samples of P44 (group III, premetaphase arrest), P9 (group IV, complete metaphase arrest), P40 (group IV), P13 (group IV), and P42 (group VI, postmetaphase arrest). Pannuclear staining is observed for P44, P9, and P42. Spermatocytes of P40 display many persistent small patches of γH2AX staining. For three other group IV patients (P13, P14, and P24) we often observed abnormal XY bodies or two (or more) γH2AX-positive XY body–like structures (see also Supplemental Fig. 3). For P13 (46,XY,inv(1)(p21q32.1)) shown here, the presence of an extra XY body–like γH2AX domain most likely represents an incompletely synapsed bivalent of chromosome 1 (due to the inversion), in addition to a normal XY body. Scale bars, 10 μm.

Enguita-Marruedo. Meiotic metaphase arrest in men. Fertil Steril 2019.

percentage of tubules with XY bodies and/or a reduced number of XY bodies per XY+T, but no significant correlation between either of these two parameters and the percentage of apoptotic metaphases was observed (%XY+T, R^2 = 0.00647, P=.6411; XY bodies/XY+T, R^2 = 0.00729, P=.6205). The most advanced spermatid types present in biopsies of patients with partial metaphase arrest (group V) were mostly early spermatids (type 2 or 3). Thus, when the SAC is frequently activated, the few cells that are able to proceed through metaphase are likely to fail in completing spermatogenesis normally.

Similar to P44 of group III (failure to reach metaphase), P9 of group IV (complete metaphase arrest) also displayed pan-chromosomal γH2AX staining indicating apoptosis in spermatocyte cells that were pre-M phase (Fig. 2D). For P40, also of group IV, frequent occurrence of multiple small patches of γH2AX in spermatocytes indicated problems in completing meiotic DNA DSB repair in (Fig. 2D). In addition, for group IV patients P13, P14, and P24 we often observed an extra XY body–like γH2AX signal in pachytene spermatocytes, which would indicate more localized chromosome pairing problems (Fig. 2D, and Supplemental Fig. 3). P13 indeed carried a large inversion in chromosome 1 (46,XY,inv(1)(p21q32.1)), but for the others karyotyping did not reveal chromosome aberrations. No such atypical γH2AX signals were detected in group V patients. From the six patients in group VI (postmetaphase arrest) we observed apoptotic nuclei in only one (P42; Fig. 2D), and no other aberrant features explaining the lack of spermatids could be observed in the other patients in this group.

Complete Metaphase Arrest and Crossover Frequency

Lack of crossover formation is a well-known trigger for SAC activation in mouse spermatocytes (43). To assess crossover frequency in group IV (complete metaphase arrest) patients, we used antibodies against MLH1 (marker of crossover sites at pachytene) (36) and SYCP3 (marker of the chromosomal axes; Fig. 3A, 3B). Two patients were excluded from the analysis, since staining for MLH1 and SYCP3 was unsuccessful. Four patients, including the three patients for whom we observed multiple XY body–like structures (P13, P14, and P24, Supplemental Fig. 3), displayed a reduced mean number of MLH1 foci (mean value range, 10–27) compared with controls (40.8 ± 5.8; Fig. 3B). We observed a negative correlation between the percentage of apoptotic metaphases and the mean number of MLH1 foci (R^2 = 0.32; P=.014; Fig. 3C).

DISCUSSION

Metaphase Arrest Is the Most Frequent Type of Male Meiotic Arrest

Herein we have shown that the metaphase checkpoint is more frequently uniformly activated than the pachytene checkpoint. This is in contrast to observations in the mouse, where knockout of genes expected to exert meiotic prophase-specific functions most frequently results in activation of one or both of the two pachytene checkpoints (9, 44). Examples are genes required for DSB formation (*Spo11, Mei4*) (45–47), for meiotic DSB repair (*Dmc1, Msh4, Msh5, Meiob*) (48–51), and/or for chromosome pairing (synaptonemal complex or cohesin components: *Sycp1, Sycp2, Sycp3, Smc1b*, and more) (52–54). Therefore, such genes might be mutated in patients displaying failure to form XY bodies. In a recent detailed study of 10 azoospermic men (32), two types of male meiotic prophase arrest were proposed, based on the absence (type I) or presence (type II) of the XY body. However, meiotic metaphase was not analyzed in this study. Since the type II patients were described to display aberrations in the expression of cell cycle genes (32), it could be worthwhile to assess whether spermatocytes in these patients might also arrest at metaphase instead of at prophase.

Metaphase arrest in mice has been observed mainly when crossover formation was affected. Mutation of genes such as *Mlh1* (6, 55) and *Rnf212* (56) almost completely abolish crossover formation. Mutation of *Shoc1* (57) or of the X-linked *Tex11* gene (58) leads to a somewhat more subtle and variable reduction in the number of crossovers (~19% for *Shoc1* and ~30% for *Tex11*), but still in combination with complete metaphase arrest. Mutations in *TEX11* have also been reported in a small percentage of men diagnosed with a meiotic arrest phenotype (59, 60). These four genes would be interesting candidates to screen for mutations in patients displaying metaphase arrest in combination with a reduction in MLH1 foci.

Still, crossover frequency was normal in most patients displaying complete metaphase arrest in this study. In these cases, alterations in other proteins involved in the metaphase-anaphase transition or functioning in cell cycle regulation may cause the observed arrest. In addition, a mild reduction in the number of crossovers (e.g., lack of the obligate crossover in the pseudoautosomal region of the XY pair), which would not result in a significant decrease in crossover frequency, could still trigger metaphase arrest in some of the patients.

Two of the patients whom we analyzed were carriers of an *AZFc* deletion. These patients are known to present variable phenotypes (ranging from Sertoli cell only to oligozoospermia) (61). In our analyses, one patient (P10) displayed failure of meiotic entry, and the other (P17) a complete metaphase arrest, confirming this variability.

Premetaphase and Postmetaphase Arrest: Novel Checkpoints or Necrosis?

In 15% of the testis biopsies we observed an arrest before meiotic metaphase (group III). Similar defects are observed in mice lacking *Hspa2*$^{-/-}$ (62), *Repro8*$^{-/-}$ (63), *Cyclin A1* (64), or *Rpl10l*, a testis-specific retrogene present in all eutherians (65). It is not known whether this lack of cells at meiotic metaphase I involves activation of a specific checkpoint or a collapse of the developmental potential of the cells after entry into meiotic prophase. Our patients in group III also displayed reduced XY body formation, indicating clear problems in reaching pachytene in addition to a failure to reach metaphase.

FIGURE 3

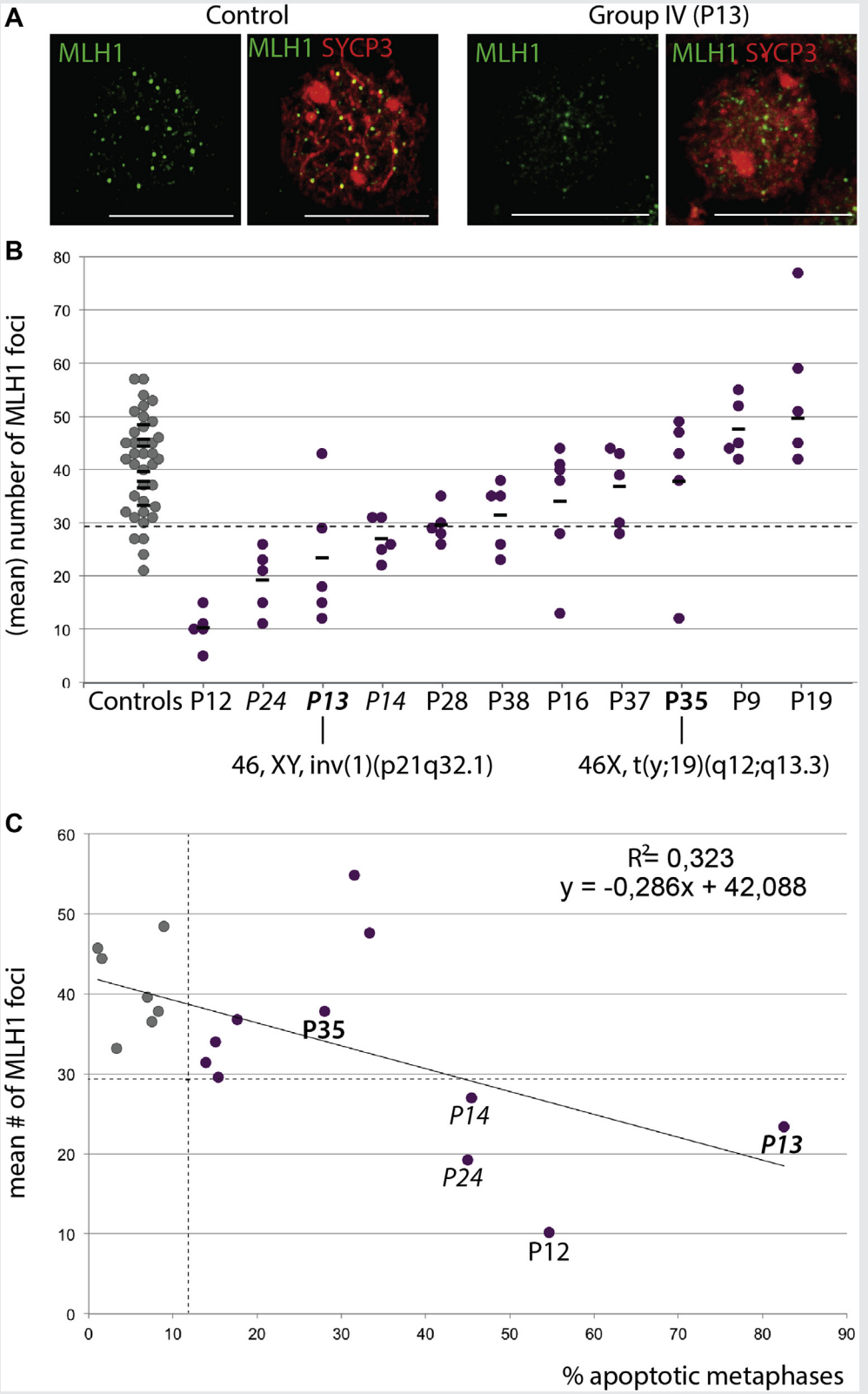

Analyses of crossover frequency. (**A**) MLH1 (green) and SYCP3 (red) in a control and patient (P13, group IV) pachytene nucleus. Scale bars, 10 μm. (**B**) Number of MLH1 foci per nucleus (dots) and mean values (horizontal bars) for each analyzed patient. (**C**) Negative correlation between the number of MLH1 foci and the percentage of apoptotic metaphases. Patient IDs for whom pachytene nuclei frequently displayed more than one XY body–like structure (Fig. 2D, Supplemental Fig. 3) are in italics; bold patient IDs indicate patients with known chromosomal aberration. The dashed line shows the threshold.

Enguita-Marruedo. Meiotic metaphase arrest in men. Fertil Steril 2019.

Postmetaphase arrest (group VI) could involve some form of cell death within a short period between the first meiotic division and early spermatid stages. Early spermatid arrest occurs in mice in which the expression of the transcription factor CREMtau has been disrupted (66). Mutation of *ZFY* could also be suspected as a cause of the failure to develop further than the meiotic divisions. In mice, *Zfy1* and *Zfy2* promote completion of meiosis II (67). In men, there is a single *ZFY* gene (68).

Since apoptotic nuclei were observed in the biopsies of only few group III and group VI patients, activation of an (apoptotic) pathway not involving pannuclear γH2AX formation (like necroptosis or necrosis) may explain the rapid loss of cells in those patients. In addition, or alternatively, malfunctioning cells may detach from the Sertoli cells, followed by sloughing into the lumen, as was previously reported for certain mouse models (69).

In conclusion, the double immunostaining with anti-γH2AX and anti-H3S10ph in combination with the decision tree we developed here is a highly feasible approach to diagnose meiotic arrest phenotypes in azoospermic men. Our approach can distinguish between failure in chromosome pairing/DSB repair and failure in the metaphase to anaphase transition. Metaphase arrest was defined as the most frequent type of meiotic arrest. Uniform activation of meiotic checkpoints suggests a genetic cause of spermatogenic arrest. Thus, this technique can also be used as a tool to preselect patients for sequencing in the search for infertility genes.

For men with nonobstructive forms of severe oligozoospermia and azoospermia, intracytoplasmic sperm injection can be used for fertility treatment, if viable spermatozoa or even spermatids can be retrieved after testicular sperm extraction (70, 71). If partial activation of meiotic checkpoints is observed in such patients, further research is recommended to determine whether the surviving gametes have increased frequencies of (epi)genetic aberrations before using them for infertility treatment.

Acknowledgments: The authors acknowledge the contributions of Prof. Dr. J. A. Grootegoed, Developmental Biology, Erasmus MC Medical Center, Rotterdam; the support during the initial phase of the project from Prof. Dr. J. Gribnau, Developmental Biology, Erasmus MC Medical Center, Rotterdam; and the advice of Dr. H. Bruggenwirth, Clinical Genetics, Erasmus MC Medical Center, Rotterdam.

REFERENCES

1. Zickler D, Kleckner N. Recombination, pairing, and synapsis of homologs during meiosis. Cold Spring Harbor Perspect Biol 2015;7:a016626.
2. Mahadevaiah SK, Turner JM, Baudat F, Rogakou EP, de Boer P, Blanco-Rodriguez J, et al. Recombinational DNA double-strand breaks in mice precede synapsis. Nat Genet 2001;27:271–6.
3. Sciurano RB, Rahn MI, Pigozzi MI, Olmedo SB, Solari AJ. An azoospermic man with a double-strand DNA break-processing deficiency in the spermatocyte nuclei: case report. Hum Reprod 2006;21:1194–203.
4. Inagaki A, Schoenmakers S, Baarends WM. DNA double strand break repair, chromosome synapsis and transcriptional silencing in meiosis. Epigenetics 2010;5:255–66.
5. Turner JM. Meiotic sex chromosome inactivation. Development 2007;134:1823–31.
6. Baker SM, Plug AW, Prolla TA, Bronner CE, Harris AC, Yao X, et al. Involvement of mouse Mlh1 in DNA mismatch repair and meiotic crossing over. Nat Genet 1996;13:336–42.
7. Barlow AL, Hulten MA. Crossing over analysis at pachytene in man. Eur J Hum Genet 1998;6:350–8.
8. Song N, Liu J, An S, Nishino T, Hishikawa Y, Koji T. Immunohistochemical analysis of histone H3 modifications in germ cells during mouse spermatogenesis. Acta Histochem Cytochem 2011;44:183–90.
9. Barchi M, Mahadevaiah S, Di Giacomo M, Baudat F, de Rooij DG, Burgoyne PS, et al. Surveillance of different recombination defects in mouse spermatocytes yields distinct responses despite elimination at an identical developmental stage. Mol Cell Biol 2005;25:7203–15.
10. Eaker S, Cobb J, Pyle A, Handel MA. Meiotic prophase abnormalities and metaphase cell death in MLH1-deficient mouse spermatocytes: insights into regulation of spermatogenic progress. Dev Biol 2002;249:85–95.
11. Faisal I, Kauppi L. Sex chromosome recombination failure, apoptosis, and fertility in male mice. Chromosoma 2016;125:227–35.
12. MacQueen AJ, Hochwagen A. Checkpoint mechanisms: the puppet masters of meiotic prophase. Trends Cell Biol 2011;21:393–400.
13. Roeder GS, Bailis JM. The pachytene checkpoint. Trends Genet 2000;16:395–403.
14. Royo H, Polikiewicz G, Mahadevaiah SK, Prosser H, Mitchell M, Bradley A, et al. Evidence that meiotic sex chromosome inactivation is essential for male fertility. Curr Biol 2010;20:2117–23.
15. Marcet-Ortega M, Pacheco S, Martinez-Marchal A, Castillo H, Flores E, Jasin M, et al. p53 and TAp63 participate in the recombination-dependent pachytene arrest in mouse spermatocytes. PLoS Genet 2017;13:e1006845.
16. Pacheco S, Marcet-Ortega M, Lange J, Jasin M, Keeney S, Roig I. The ATM signaling cascade promotes recombination-dependent pachytene arrest in mouse spermatocytes. PLoS Genet 2015;11:e1005017.
17. Marston AL, Wassmann K. Multiple duties for spindle assembly checkpoint kinases in meiosis. Frontiers Cell Dev Biol 2017;5:109.
18. Musacchio A. The molecular biology of spindle assembly checkpoint signaling dynamics. Curr Biol 2015;25:R1002–18.
19. Sun SC, Kim NH. Spindle assembly checkpoint and its regulators in meiosis. Hum Reprod Update 2012;18:60–72.
20. Foresta C, Ferlin A, Bettella A, Rossato M, Varotto A. Diagnostic and clinical features in azoospermia. Clin Endocrinol 1995;43:537–43.
21. Guichaoua MR, Perrin J, Metzler-Guillemain C, Saias-Magnan J, Giorgi R, Grillo JM. Meiotic anomalies in infertile men with severe spermatogenic defects. Hum Reprod 2005;20:1897–902.
22. Hann MC, Lau PE, Tempest HG. Meiotic recombination and male infertility: from basic science to clinical reality? Asian J Androl 2011;13:212–8.
23. Martin-du Pan RC, Campana A. Physiopathology of spermatogenic arrest. Fertil Steril 1993;60:937–46.
24. North MO, Lellei I, Erdei E, Barbet JP, Tritto J. Meiotic studies of infertile men in case of non-obstructive azoospermia with normal karyotype and no microdeleted Y-chromosome precise the clinical couple management. Ann Genet 2004;47:113–23.
25. Sun F, Turek P, Greene C, Ko E, Rademaker A, Martin RH. Abnormal progression through meiosis in men with nonobstructive azoospermia. Fertil Steril 2007;87:565–71.
26. Tesarik J, Greco E, Cohen-Bacrie P, Mendoza C. Germ cell apoptosis in men with complete and incomplete spermiogenesis failure. Mol Hum Reprod 1998;4:757–62.
27. Topping D, Brown P, Judis L, Schwartz S, Seftel A, Thomas A, et al. Synaptic defects at meiosis I and non-obstructive azoospermia. Hum Reprod 2006;21:3171–7.
28. Weedin JW, Bennett RC, Fenig DM, Lamb DJ, Lipshultz LI. Early versus late maturation arrest: reproductive outcomes of testicular failure. J Urol 2011;186:621–6.
29. Codina-Pascual M, Oliver-Bonet M, Navarro J, Campillo M, Garcia F, Egozcue S, et al. Synapsis and meiotic recombination analyses: MLH1 focus in the XY pair as an indicator. Hum Reprod 2005;20:2133–9.
30. Sciurano RB, Rahn MI, Rey-Valzacchi G, Coco R, Solari AJ. The role of asynapsis in human spermatocyte failure. Int J Androl 2012;35:541–9.

31. Vidal F, Templado C, Navarro J, Brusadin S, Marina S, Egozcue J. Meiotic and synaptonemal complex studies in 45 subfertile males. Hum Genet 1982;60: 301–4.
32. Jan SZ, Jongejan A, Korver CM, van Daalen SKM, van Pelt AMM, Repping S, et al. Distinct prophase arrest mechanisms in human male meiosis. Development 2018;145:dev160614.
33. Ben Khelifa M, Ghieh F, Boudjenah R, Hue C, Fauvert D, Dard R, et al. A MEI1 homozygous missense mutation associated with meiotic arrest in a consanguineous family. Hum Reprod 2018;33:1034–7.
34. Gershoni M, Hauser R, Barda S, Lehavi O, Arama E, Pietrokovski S, et al. A new MEIOB mutation is a recurrent cause for azoospermia and testicular meiotic arrest. Hum Reprod 2019;34:666–71.
35. Tuttelmann F, Ruckert C, Ropke A. Disorders of spermatogenesis: perspectives for novel genetic diagnostics after 20 years of unchanged routine. Med Genet 2018;30:12–20.
36. Riera-Escamilla A, Enguita-Marruedo A, Moreno-Mendoza D, Chianese C, Sleddens-Linkels E, Contini E, et al. Sequencing of a "mouse azoospermia" gene panel in azoospermic men: identification of RNF212 and STAG3 mutations as novel genetic causes of meiotic arrest. Hum Reprod 2019;34:978–88.
37. Johnsen SG. Testicular biopsy score count—a method for registration of spermatogenesis in human testes: normal values and results in 335 hypogonadal males. Hormones 1970;1:2–25.
38. Dohle GR, Halley DJ, Van Hemel JO, van den Ouwel AM, Pieters MH, Weber RF, et al. Genetic risk factors in infertile men with severe oligozoospermia and azoospermia. Hum Reprod 2002;17:13–6.
39. Lammers JH, Offenberg HH, van Aalderen M, Vink AC, Dietrich AJ, Heyting C. The gene encoding a major component of the lateral elements of synaptonemal complexes of the rat is related to X-linked lymphocyte-regulated genes. Mol Cell Biol 1994;14:1137–46.
40. Moore HD, Smith CA, Hartman TD, Bye AP. Visualization and characterization of the acrosome reaction of human spermatozoa by immunolocalization with monoclonal antibody. Gamete Res 1987;17:245–9.
41. Schindelin J, Arganda-Carreras I, Frise E, Kaynig V, Longair M, Pietzsch T, et al. Fiji: an open-source platform for biological-image analysis. Nat Methods 2012;9:676–82.
42. Solier S, Pommier Y. The nuclear gamma-H2AX apoptotic ring: implications for cancers and autoimmune diseases. Cell Mol Life Sci 2014;71:2289–97.
43. Gorbsky GJ. The spindle checkpoint and chromosome segregation in meiosis. FEBS J 2015;282:2471–87.
44. de Rooij DG, de Boer P. Specific arrests of spermatogenesis in genetically modified and mutant mice. Cytogenet Genome Res 2003;103:267–76.
45. Baudat F, Manova K, Yuen JP, Jasin M, Keeney S. Chromosome synapsis defects and sexually dimorphic meiotic progression in mice lacking spo11. Mol Cell 2000;6:989–98.
46. Romanienko PJ, Camerini-Otero RD. The mouse spo11 gene is required for meiotic chromosome synapsis. Mol Cell 2000;6:975–87.
47. Kumar R, Bourbon HM, de Massy B. Functional conservation of Mei4 for meiotic DNA double-strand break formation from yeasts to mice. Genes Dev 2010;24:1266–80.
48. Pittman DL, Cobb J, Schimenti KJ, Wilson LA, Cooper DM, Brignull E, et al. Meiotic prophase arrest with failure of chromosome synapsis in mice deficient for Dmc1, a germline-specific RecA homolog. Mol Cell 1998;1:697–705.
49. Kneitz B, Cohen PE, Avdievich E, Zhu L, Kane MF, Hou H Jr, et al. MutS homolog 4 localization to meiotic chromosomes is required for chromosome pairing during meiosis in male and female mice. Genes Dev 2000;14:1085–97.
50. de Vries SS, Baart EB, Dekker M, Siezen A, de Rooij DG, de Boer P, et al. Mouse MutS-like protein Msh5 is required for proper chromosome synapsis in male and female meiosis. Genes Dev 1999;13:523–31.
51. Yang F, De La Fuente R, Leu NA, Baumann C, McLaughlin KJ, Wang PJ. Mouse SYCP2 is required for synaptonemal complex assembly and chromosomal synapsis during male meiosis. J Cell Biol 2006;173:497–507.
52. de Vries FA, de Boer E, van den Bosch M, Baarends WM, Ooms M, Yuan L, et al. Mouse Sycp1 functions in synaptonemal complex assembly, meiotic recombination, and XY body formation. Genes Dev 2005; 19:1376–89.
53. Kouznetsova A, Novak I, Jessberger R, Hoog C. SYCP2 and SYCP3 are required for cohesin core integrity at diplotene but not for centromere cohesion at the first meiotic division. J Cell Sci 2005;118:2271–8.
54. Hamer G, Novak I, Kouznetsova A, Hoog C. Disruption of pairing and synapsis of chromosomes causes stage-specific apoptosis of male meiotic cells. Theriogenology 2008;69:333–9.
55. Edelmann W, Cohen P, Kane M, Lau K, Morrow B, Bennett S, et al. Meiotic pachytene arrest in MLH1-deficient mice. Cell 1996;85:1125–34.
56. Reynolds A, Qiao H, Yang Y, Chen JK, Jackson N, Biswas K, et al. RNF212 is a dosage-sensitive regulator of crossing-over during mammalian meiosis. Nat Genet 2013;45:269–78.
57. Guiraldelli MF, Felberg A, Almeida LP, Parikh A, de Castro RO, Pezza RJ. SHOC1 is a ERCC4-(HhH)2-like protein, integral to the formation of crossover recombination intermediates during mammalian meiosis. PLoS Genet 2018;14:e1007381.
58. Yang F, Gell K, van der Heijden GW, Eckardt S, Leu NA, Page DC, et al. Meiotic failure in male mice lacking an X-linked factor. Genes Dev 2008; 22:682–91.
59. Yang F, Silber S, Leu NA, Oates RD, Marszalek JD, Skaletsky H, et al. TEX11 is mutated in infertile men with azoospermia and regulates genome-wide recombination rates in mouse. EMBO Mol Med 2015;7:1198–210.
60. Yatsenko AN, Georgiadis AP, Ropke A, Berman AJ, Jaffe T, Olszewska M, et al. X-linked TEX11 mutations, meiotic arrest, and azoospermia in infertile men. N Engl J Med 2015;372:2097–107.
61. Krausz C, Casamonti E. Spermatogenic failure and the Y chromosome. Hum Genet 2017;136:637–55.
62. Dix DJ, Allen JW, Collins BW, Poorman-Allen P, Mori C, Blizard DR, et al. HSP70-2 is required for desynapsis of synaptonemal complexes during meiotic prophase in juvenile and adult mouse spermatocytes. Development 1997;124:4595–603.
63. Sun F, Palmer K, Handel MA. Mutation of Eif4g3, encoding a eukaryotic translation initiation factor, causes male infertility and meiotic arrest of mouse spermatocytes. Development 2010;137:1699–707.
64. Nickerson HD, Joshi A, Wolgemuth DJ. Cyclin A1-deficient mice lack histone H3 serine 10 phosphorylation and exhibit altered aurora B dynamics in late prophase of male meiosis. Dev Biol 2007;306:725–35.
65. Jiang L, Li T, Zhang X, Zhang B, Yu C, Li Y, et al. RPL10L is required for male meiotic division by compensating for RPL10 during meiotic sex chromosome inactivation in mice. Curr Biol 2017;27:1498–505.e6.
66. Nantel F, Monaco L, Foulkes NS, Masquillier D, LeMeur M, Henriksen, et al. Spermiogenesis deficiency and germ-cell apoptosis in *CREM*-mutant mice. Nature 1996;380:159–65.
67. Vernet N, Mahadevaiah SK, Yamauchi Y, Decarpentrie F, Mitchell MJ, Ward MA, et al. Mouse Y-linked Zfy1 and Zfy2 are expressed during the male-specific interphase between meiosis I and meiosis II and promote the 2nd meiotic division. PLoS Genet 2014;10:e1004444.
68. Decarpentrie F, Vernet N, Mahadevaiah SK, Longepied G, Streichemberger E, Aknin-Seifer I, et al. Human and mouse ZFY genes produce a conserved testis-specific transcript encoding a zinc finger protein with a short acidic domain and modified transactivation potential. Hum Mol Gen 2012;21:2631–45.
69. Yan W. Male infertility caused by spermiogenic defects: lessons from gene knockouts. Mol Cell Endocrinol 2009;306:24–32.
70. Devroey P, Liu J, Nagy Z, Goossens A, Tournaye H, Camus M, et al. Pregnancies after testicular sperm extraction and intracytoplasmic sperm injection in non-obstructive azoospermia. Hum Reprod 1995;10:1457–60.
71. Tanaka A, Suzuki K, Nagayoshi M, Tanaka A, Takemoto Y, Watanabe S, et al. Ninety babies born after round spermatid injection into oocytes: survey of their development from fertilization to 2 years of age. Fertil Steril 2018; 110:443–51.

El bloqueo meiótico sucede más frecuentemente durante la metafase y a menudo es incompleta en hombres azoospérmicos

Objetivo: Establecer qué puntos de control meióticos son activados en varones con alteración grave en la espermatogénesis para mejorar la caracterización fenotípica de anomalías meióticas.

Diseño: Estudio retrospectivo observacional.

Lugar: Laboratorio de investigación de centro médico universitario y clínica de andrología.

Pacientes: Cuarenta y ocho pacientes con alteraciones graves en la espermatogénesis confirmadas (puntuación Johnsen 3-6) y 15 controles (puntuación Jonhsen 10).

Intervenciones: Ninguna.

Resultados principales: Evaluación cuantitativa del análisis de inmunofluorescencia de marcadores específicos para determinar el inicio de la meiosis, el apareamiento de cromosomas, la progresión de la reparación de la rotura de doble cadena del ADN, la formación del entrecruzamiento, la formación de metafases meióticas, el bloqueo de la metafase y la formación de espermátides, dando como resultado una nueva clasificación de tipos de bloqueos meióticos humanos.

Resultado(s): El bloqueo completo metafásico fue el fenómeno más frecuente (27%), los pacientes con el porcentaje de metafases apoptótico más elevado también mostraron una reducción en el número de quiasmas. Se observó un bloqueo incompleto de la metafase en un 17% de los pacientes. Solo cuatro pacientes (8%) fueron incapaces de finalizar el apareamiento meiótico de cromosomas provocando un bloqueo en paquitene. Se definieron dos nuevos tipos de bloqueo meiótico: bloqueo en pre-metafase y post-metafase (15% y 13%, respectivamente).

Conclusión(es): El bloqueo meiótico en hombres sucede con mayor frecuencia durante la metafase meiótica. Este bloqueo puede ser incompleto, dando como resultado un bajo número de espermátides y a menudo ocurre asociado a una menor frecuencia de entrecruzamientos. El enfoque fenotípico aquí descrito proporciona una visión mecanicista para ayudar a identificar genes responsables de la infertilidad y para evaluar las correlaciones genotipo – fenotipo en casos particulares.

SUPPLEMENTAL FIGURE 1

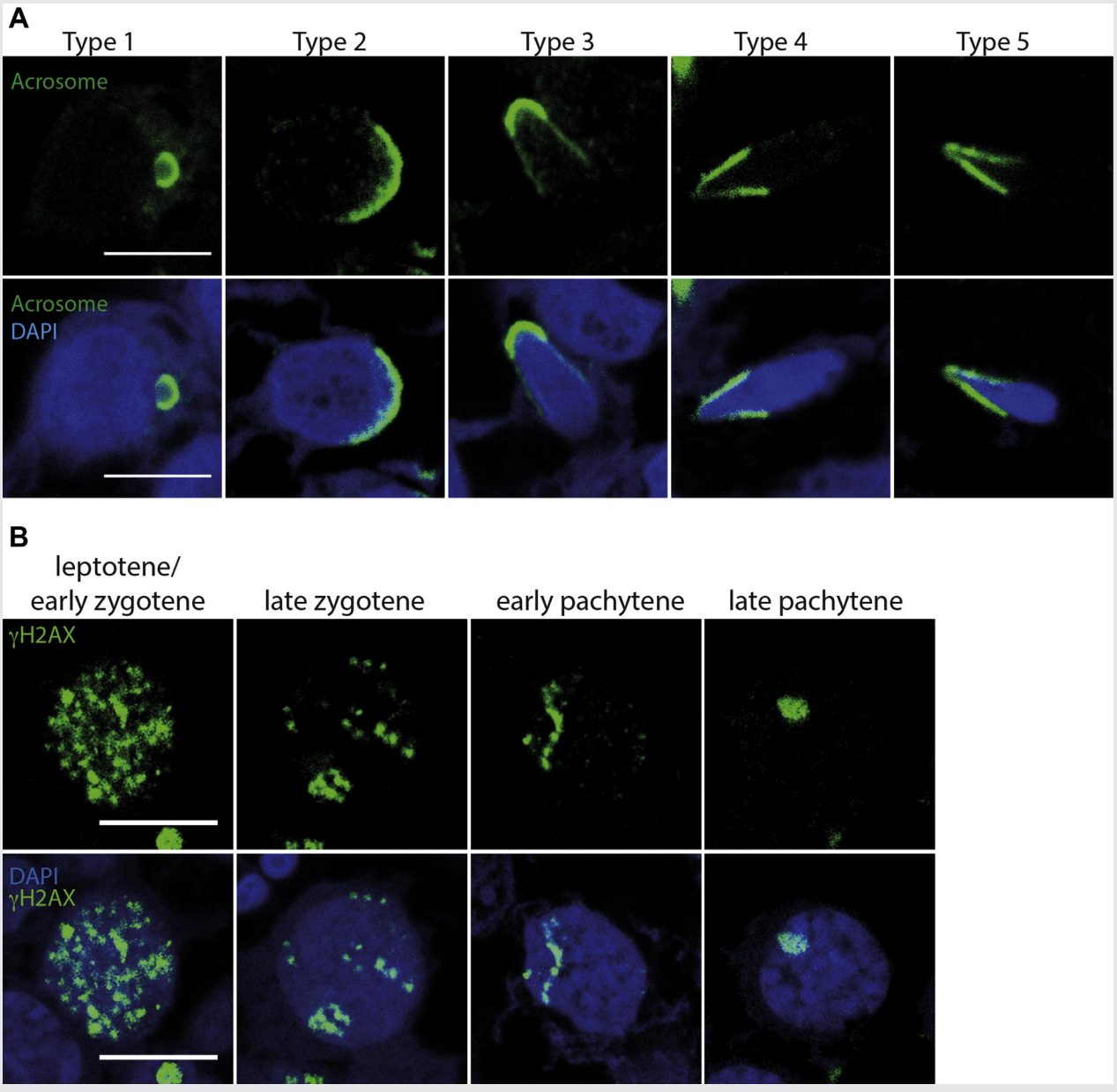

Identification of spermatocyte and spermatid substages. (**A**) Types of spermatids identified in control sample. (**B**) Meiotic prophase stages present in controls (late zygotene and late pachytene nuclei are magnifications of the nuclei indicated in Fig. 1A). Immunostained antigens are as indicated on the images. Scale bar, 10 μm.

Enguita-Marruedo. Meiotic metaphase arrest in men. Fertil Steril 2019.

SUPPLEMENTAL FIGURE 2

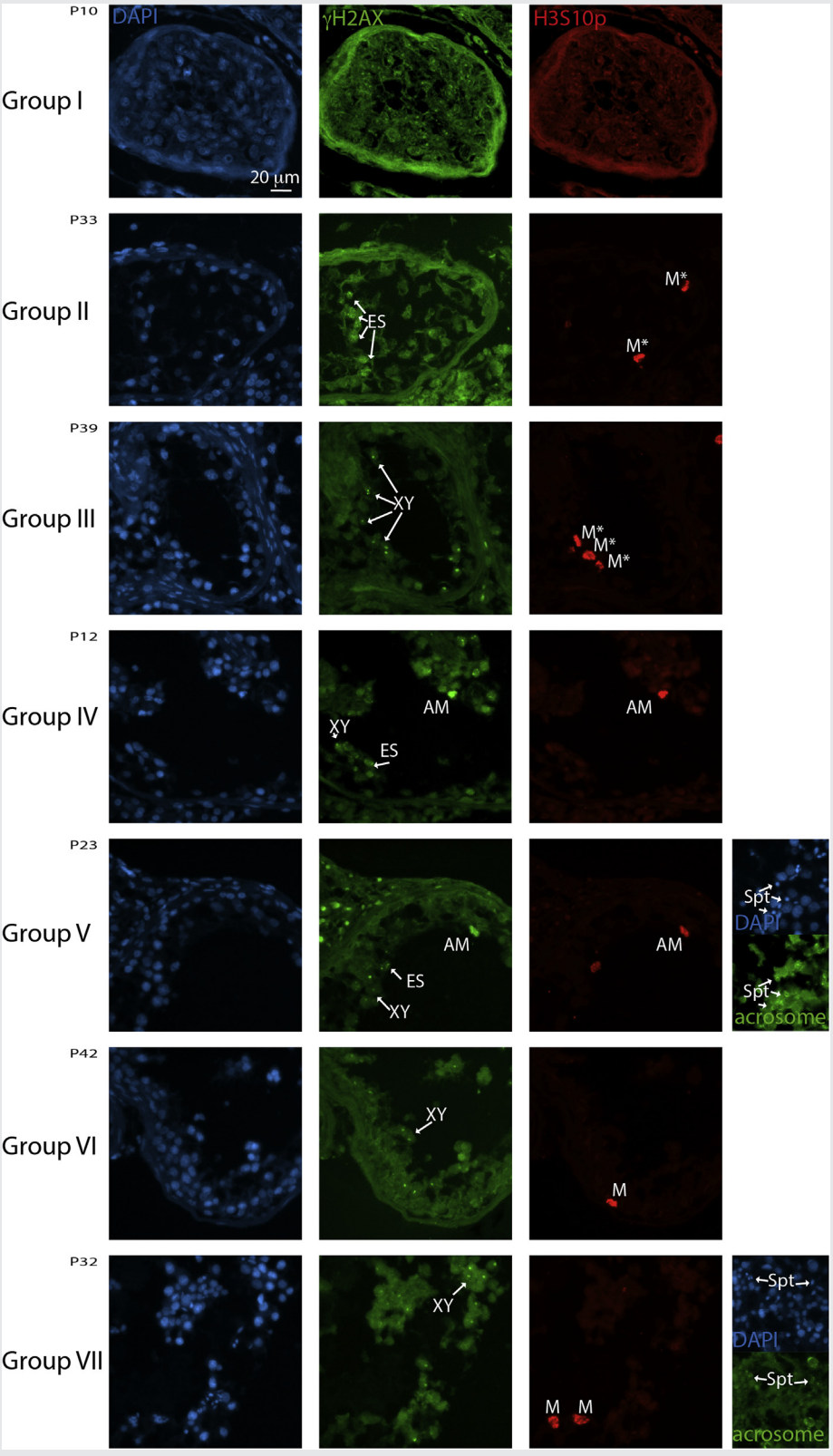

Example overview images of representatives from each patient group. Representative widefield immunofluorescent images of each patient grouped as indicated. Patient numbers are shown. Blue (DAPI) green (γH2AX or acrosome as indicated) and red (H3S10p) immunofluorescent signals are shown separately. Examples of early spermatocytes (ES), pachytene spermatocytes (XY), mitotic (M*) and (apoptotic) meiotic metaphases ((A) M), and spermatids (Spt) are indicated with arrows. Scale bar, 20 μm.

Enguita-Marruedo. Meiotic metaphase arrest in men. Fertil Steril 2019.

SUPPLEMENTAL FIGURE 3

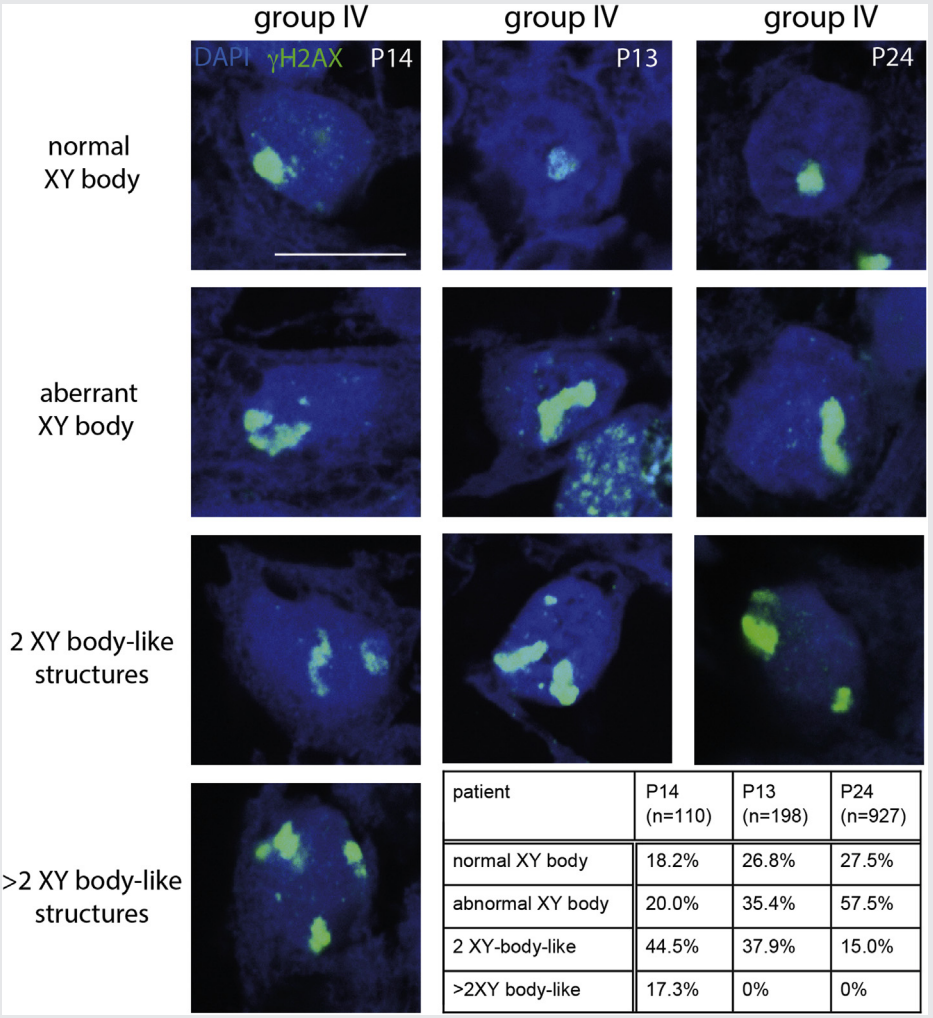

patient	P14 (n=110)	P13 (n=198)	P24 (n=927)
normal XY body	18.2%	26.8%	27.5%
abnormal XY body	20.0%	35.4%	57.5%
2 XY-body-like	44.5%	37.9%	15.0%
>2XY body-like	17.3%	0%	0%

Aberrant XY body–like structures in some group IV patients. Pachytene nuclei from three patients with aberrant XY body–like structures; P14, P13 (46XY, inv(1)(p21q32.1)), and P24, all displaying varying frequencies of aberrant XY body–like structures, as indicated in Table 1 (lower right corner). The variable "n" indicates the number of nuclei that were analyzed. All three patients also displayed a reduction in the average MLH1 foci number (Fig. 3). Scale bars, 10 μm.

Enguita-Marruedo. Meiotic metaphase arrest in men. Fertil Steril 2019.